Robustness Analysis of Face Obscuration

Hanxiang Hao[1], David Güera[1], János Horváth[1], Amy R. Reibman[2], Edward J. Delp[1]

[1] Video and Image Processing Lab (VIPER), Purdue University, West Lafayette, Indiana USA

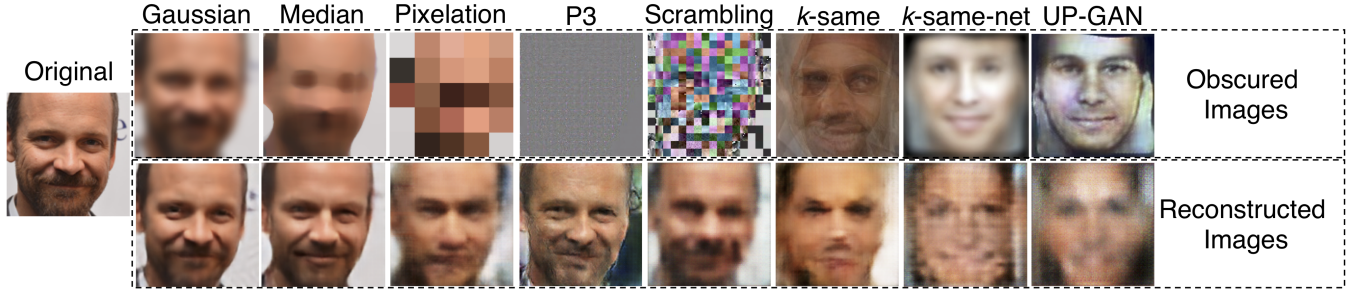[2] School of Electrical and Computer Engineering, Purdue University, West Lafayette, Indiana USA

Fig. 1: Reconstruction of obscured images using Pix2Pix [10] as described in Section III-D. Although the obscured images are hard to recognize, deep learning models can still recover the person's identity. For Gaussian, median, and P3, we can clearly recognize the person from their recovered images.

Abstract—**Face obscuration is needed by law enforcement and mass media outlets to guarantee privacy. Sharing sensitive content where obscuration or redaction techniques have failed to completely remove all identifiable traces can lead to many legal and social issues. Hence, we need to be able to systematically measure the face obscuration performance of a given technique. In this paper we propose to measure the effectiveness of eight obscuration techniques. We do so by attacking the redacted faces in three scenarios: obscured face identification, verification, and reconstruction. Threat modeling is also considered to provide a vulnerability analysis for each studied obscuration technique. Based on our evaluation, we show that the k-same based methods are the most effective.**

I. INTRODUCTION

From TV news to Google StreetView, object obscuration has been used in many applications to provide privacy protection. Law enforcement agencies use obscuration techniques to avoid exposing the identities of bystanders or officers. To remove identifiable information, Gaussian blurring or pixelation methods are commonly used. Median filtering is also used due to its simple implementation and its non-linearity, which translates into higher information distortion when compared to linear filters such as the Gaussian filter. These simple obscuration techniques are able to successfully prevent humans from recognizing the obscured objects. Previous work [5], [14], [23] shows that machine learning approaches can still identify these objects using the subtle information left in the obscured images. More robust and effective techniques have been described including k-same methods [17], [7], [4], [15], [8] which are able to provide a secured obscuration while preserving non-identifiable information. Reversible obscuration [22], [20], [35] is another type of method to prevent the leakage of privacy information from unauthorized viewers when sharing an image on social media. This type of methods is designed to achieve privacy-preserving image sharing by encrypting the images published on the Internet. Only the viewer with the correct decoding key is able to access the image. In this paper, we focus on the robustness analysis of several obscuration techniques for face redaction. We study these obscuration methods to answer the following question: "Is there any remaining identifiable information from the obscured faces to enable re-identification?".

Although several of these approaches are widely used by news outlets, social media platforms, and government agencies, their performance has not been objectively measured. The lack of a formal study of these obscuration techniques makes it hard to evaluate the quality of redaction systems. As shown by McPherson *et al.* [14], a deep learning model with a simple structure is able to identify individuals from their highly pixelated and blurred faces. This indicates that human perception is no longer the gold standard to examine the effectiveness of obscuration methods. To provide a better way to examine a given obscuration method, we need to consider it in a controlled environment that can determine how well identifiable information can be extracted from the obscured face. We design three scenarios: obscured face identification, verification, and reconstruction. Figure 1 shows the results from the reconstruction attack for the eight studied obscuration methods. To analyze the vulnerability of these obscuration methods, we also examine multiple threat models based on an attacker's knowledge of the obscuration method used. Our simplest threat model assumes that the attacker has no information of these obscuration methods. In the most challenging threat scenario, we consider that the attacker knows the exact type of the obscuration method and its hyperparameters. These previously unexplored threat models are necessary to offer a complete vulnerability analysis under realistic situations.

The main contributions of this paper are summarized as follows. First, we design three attack scenarios: obscured face identification, verification, and reconstruction. We also analyze these attacks based on two widely used deep learning models, VGG19[27] and ResNet50[9] in different threat model conditions. Finally, we provide a comprehensive robustness analysis of eight obscuration methods. These methods include three traditional methods (Gaussian blurring, median blurring, and pixelation), three k-same based methods (k-same [7], k-same-net [15], and UP-GAN [8]) and two privacy-preserving image sharing methods (P3 [22] and scrambling [35]).

II. RELATED WORK

Face Obscuration Methods. As previously mentioned, Gaussian blurring and pixelation are frequently used in many applications. However, these techniques are not reliable. As we will show in Section IV, Gaussian blurring even with a large kernel size is still not able to defend against the some of our attacks. An extreme example of blurring to prevent information leaking is to simply gray out the entire facial region by setting all pixels in the facial area to a fixed value. This approach is rarely used because its visual effect is unpleasant, especially if there are many faces in the scene that need to be redacted.

To address some of these issues, k-same methods [17], [7], [4], [15], [8] have been proposed to balance the removal of identifiable information while preserving non-identifiable facial features. These methods attempt to group faces into clusters based on personal attributes such as age, gender, or facial expression. Then, a template face for each cluster is generated. These methods can fulfill the requirement of k-anonymity [24]. More specifically, they are able to guarantee that any face recognition system cannot do better than $1/k$ in recognizing to whom a particular image corresponds, where k is the minimum number of faces among all clusters [7]. In Newton *et al*. [17] and Gross *et al*. [7], they simply compute the average face for each cluster. Therefore, the obscured faces are blurry and cannot handle various facial poses. Du *et al*. [4] use the active appearance model [2] to learn the shape and appearance of faces. Then, they generate a template face for each cluster to produce obscured faces with better visual quality. A generative neural network, k-same-net, that directly generates faces based on the cluster attributes is described in [15]. To produce more realistic faces, generative adversarial network (GAN) [6] have been used, since its discriminator is designed to guide the generator by distinguishing real faces from generated faces. Hao *et al*. [8] propose a method based on conditional GAN [16] that can generate a synthetic face given the facial landmarks and cluster attributes without the original image.

Besides the methods above that permanently remove the identifiable information, reversible obscuration methods [22], [20], [35] are also needed for the purposes of privacy-preserving image sharing. These reversible obscuration methods split the image information into two parts: 1) the public part which contains most volume, but not meaningful content

and 2) a secret part that stores the image decoding key. Therefore, when publishing an image to social media, the public and secret parts can be stored separately to avoid the leakage of images to unauthorized viewers. Ra *et al*. [22] propose a method, P3, which is based on the JPEG encoding framework. They separate the DCT coefficients in the JPEG encoding process based on a predefined threshold value to generate the public and secret images. Yuan *et al*. [35] propose a scrambling method that further reduces the data storage in the secret part. Instead of thresholding, they randomly flip the the sign of DCT coefficients and store the result as the public image. For the secret part, they only need to store the random seed to recover the original image.

Privacy Analysis of Obscuration Methods. Dufaux and Ebrahimi, and Sah *et al*. [5], [23] provide an analysis of the obscuration performance of simple identifiers and show the ineffectiveness of current obscuration methods. By using a simple deep learning model, McPherson *et al*. [14] also show that obscured images still contain enough information to perform accurate identification. They uncover the identity obscured with blurring, pixelation, and P3 methods. Oh *et al*. [19] also propose a semi-supervised model that is able to identify the face under large variations in pose.

To extend the previous literature [5], [23], [14], [19], we first consider the face identification scenario. By mapping faces to known identities in different threat models, we analyze the vulnerability of each obscuration method using advanced deep learning identification methods. However, the requirement of known identities weakens this type of analysis, since query faces usually come from unknown identities. To overcome this, we provide a threat analysis under a more realistic setup: the face verification scenario. Specifically, we want to measure the similarity of an unknown redacted face to clear target faces. Since it allows recognizing unseen identities, this scenario is more realistic. Lastly, a reconstruction scenario is proposed to visualize how well we can recover the true identity using the remaining information from the obscured images.

III. PROPOSED METHOD

To evaluate the performance of the obscuration methods, we first introduce the three threat models based on the amount of knowledge about the obscuration method that is available to the attackers. Then we describe the three attacks: obscured face identification, verification, and reconstruction.

A. Threat Modeling

In our model, the attacker aims to identify the redacted faces based on the information still present in the obscured images. We design three threat models, which vary on how much information about the used obscuration approach is available to the attacker.

- Threat model T_1 assumes the attacker has no information of any obscuration method, which means that the attacker is only able to learn the facial features used for identification from clear faces. During the testing

phase, it extracts the facial features from the obscured faces directly.

- Threat model T_2 assumes the attacker is aware of some obscuration methods, but not the same method used in the testing phase. *i.e.* the attacker is trained on both clear and obscured images and tested with the obscured images of the obscuration methods not used in the training set. This model provides more information to the attacker, since different obscuration methods may share similarities in terms of identifying facial features. Introducing the obscured images serves the same role as data augmentation.
- Threat model T_3 assumes the attacker knows the exact type of the obscuration method and its hyperparameters, like the kernel size of Gaussian blurring. Compared to T_1 and T_2, T_3 is the strongest and most realistic attack, since it provides the attacker with the most information of the obscuration method to identify identities.

B. Obscured Face Identification Attack

For the obscured face identification attack, we assume a fixed number of identities. We treat this identification problem as a classification problem where the number of classes is equal to the number of identities. In this paper, we evaluate the performance of different obscuration methods based on different backbone deep learning models, such as VGG19 or ResNet50 in order to have a more generalizable conclusion.

C. Obscured Face Verification Attack

The obscured face verification attack is defined as: given an obscured face and a clear face, decide if the two faces come from the same person or not. Previous work [5], [23], [14], [19] only considers the identification scenario, which assumes all identities are in the dataset. However, in many cases, we cannot assume the obscured identity is in any dataset. For example, the attackers may want to find out if the obscured face from a TV news is a person they know. Therefore, face verification attack is more stringent.

In order to solve this verification problem, we project the image into a low-dimension latent vector, where faces from the same person are closer together than faces from different people. Therefore, by comparing the distance of the latent vectors, we can determine if the two faces are from the same person or not. To improve the accuracy, we use the Additive Angular Margin loss (also known as ArcFace) [3] to obtain highly discriminative features for face recognition. ArcFace simultaneously reduces intra-class difference and enlarge inter-class difference of the embedding vectors. We choose ArcFace because it yields the best facial recognition performance among the traditional softmax loss [32], [29], [1], contrastive loss [28], [31], [30], triplet loss [21], [26], [25], and other angular space losses, like SphereFace [13], [12] and CosFace [34], [33]. Specifically, ArcFace is designed to enforce a margin between the distance of the sample to its class center and the distances of the sample to the other centers from different classes in angular space.

Given an input image (either clear image or obscured image), we first embed it as a low-dimension vector $\mathbf{x} \in \mathbb{R}^d$ using a deep learning model. Define an auxiliary projection weight $\mathbf{W} \in \mathbb{R}^{d \times n}$, where n is the number of unique identities in the dataset. We further normalize the embedding vector and projection weight as $\hat{\mathbf{x}} = \frac{\mathbf{x}}{\|\mathbf{x}\|}$ and $\hat{\mathbf{W}} = \frac{\mathbf{W}}{\|\mathbf{W}\|}$, respectively. The normalized embedding vector then is projected onto $\mathbb{R}^n$ as follows

$$\hat{\mathbf{W}}^T \hat{\mathbf{x}} = \|\hat{\mathbf{W}}\| \|\hat{\mathbf{x}}\| \cos \boldsymbol{\theta} = \cos \boldsymbol{\theta},$$

where $\boldsymbol{\theta} \in \mathbb{R}^n$ is a vector of angular distance from $\hat{\mathbf{x}}$ to $\hat{\mathbf{W}}$. The normalized embedding vector is then re-scaled by multiplying a scalar s to make it distributed on a hypersphere with a radius of s. The ArcFace loss function of a single sample is then calculated using softmax cross entropy as follows

$$L = -\log \frac{e^{s \cos(\theta_t + m)}}{e^{s \cos(\theta_t + m)} + \sum_{j=1, j \neq t}^{n} e^{s \cos(\theta_j)}},$$

where m is the additive angular margin penalty between $\mathbf{x}$ and $\mathbf{W}$, θ_t is the angle of the target class of the input image. Note that the computation of the ArcFace loss is only used to aid the training process. For inference, we compute the embedding vectors from the clear face $\boldsymbol{x}_c$ and obscured face $\boldsymbol{x}_o$ using the same deep learning model. We then compare the angular distance after normalization to a predefined threshold value to determine the verification result. The threshold value can be obtained based on the value that maximizes the verification accuracy on the validation set.

D. Obscured Face Reconstruction

As we will show in Section IV, highly obscured images still contain identifiable information. To examine the amount of remaining information in obscured images, we design a reconstruction attack to visualize how well we can recover the original image. We apply a conditional generative adversarial network, Pix2Pix [10], to perform this image reconstruction attack. Given the obscured images, the generator is trained to reconstruct the clear image guided by the discriminator and the L_2 distance loss. To quantify the reconstruction performance, we compute the mean square error (MSE) over pixel-wise differences. We also compute the identification accuracy based on a face recognition model which is pretrained with clear images. This test provides us a way to quantify and visualize the amount of identifiable information leaked from the obscuration methods.

IV. EXPERIMENTS

In this section, we first briefly describe the obscuration methods to be evaluated. Then, we provide the design and result of the aforementioned attacking scenarios.

A. Evaluated Methods

In this work, we propose to analyze eight obscuration methods. These methods include three traditional methods (Gaussian blurring, median blurring, and pixelation), three k-same based methods (k-same, k-same-net, and UP-GAN)

and two privacy-preserving image sharing methods (P3 and scrambling). Examples of obscured faces using these methods are shown in Figure 1. We use Gaussian-5 representing the experiment of Gaussian blurring with kernel size of 5.

Traditional obscuration methods. We evaluate the three obscuration methods including Gaussian blurring, median blurring and pixelation methods for four different kernel (pixel) sizes of 5, 15, 25, and 35. We use the OpenCV function *cv2.getGaussianKernel* to compute the kernel of Gaussian blurring. Note that the Gaussian standard deviation is defined as

$$\sigma = 0.3 * \left(\left(\frac{w-1}{2} - 1 \right) + 0.8 \right),$$

where w is the kernel size. The pixelation method is implemented by image downsampling and upsampling using nearest-neighbor interpolation.

k-same based obscuration methods. k-same based methods aim to obscure identifiable information while preserving the non-identifiable information (also known as utility information). Algorithm 1 shows the workflow of the k-same based methods, which is based on [7]. In this work, we choose $k = 10$. We evaluate three k-same based methods: the original k-same method [7], k-same-net [15], and UP-GAN [8]. We model the obscuration process as follows.

Suppose we have a clear face dataset $\mathcal{M}_c$ and an obscuration function f mapping the clear image I_c to the obscured image I_o by $I_o = f(I_c)$. We use this mapping function building an obscured face dataset $\mathcal{M}_o$ based on $\mathcal{M}_c$. Based on [7], we also need to assume the dataset $\mathcal{M}_c$ has no two images coming from the same identity to make Algorithm 1 k-anonymous. The k-same based methods require the function f mapping k nearest neighbors from the clear images to a single obscured image. For example, considering the original k-same method, the obscured face is obtained by averaging the k nearest neighbors in the image space. Therefore, the $x_{1,...,k}$ from Algorithm 1 in this case are the clear images.

k-same-net is a generative deep learning model that generates fake faces given the cluster attributes. UP-GAN has similar generator architecture to k-same-net with the same input cluster attributes. However, it improves the generated image quality using its discriminator and the perceptual loss constraint. For both k-same-net and UP-GAN, the $x_{1,...,k}$ from Algorithm 1 are the cluster attributes. Therefore, the input attribute to the models is the average of the k nearest neighbors in the attribute space.

As proposed by [8], we choose UTKFace dataset [36], which contains the required utility values (age, gender, and skin tone) and facial landmarks to train k-same-net and UP-GAN. The utility values are defined as facial features that do not reveal identity, such as age, gender, skin tone, pose, and expression [8]. For the purpose of obscuration evaluation, we test these two methods on the FaceScrub dataset [18], with a fixed utility values (26 years old, male, and white)

Algorithm 1: Workflow of the k-same based methods.

Input: Clear face dataset $\mathcal{M}_c$, privacy constant k with $|\mathcal{M}_c| \geq k$
Output: Obscured face dataset $\mathcal{M}_o$
$\mathcal{M}_o \leftarrow \emptyset$;
for $i \in \mathcal{M}_c$ **do**
  if $|\mathcal{M}_c| < k$ **then**
    $k = |\mathcal{M}_c|$;
  end
  Select the k nearest neighbors $x_1, \ldots, x_k \in \mathcal{M}_c$;
  $x_o \leftarrow \frac{\sum_{m=1}^{k} x_m}{k}$;
  Add k copies of x_o to $\mathcal{M}_o$;
  Remove $x_1, \ldots, x_k$ from $\mathcal{M}_c$;
end

---

and 7-point facial landmarks obtained by *Dlib* toolkit [11][1]. These points include the centers of the eyes, the center of the nose, and four points around the mouth. Note that since the FaceScrub dataset contains different faces from the same identity, the k-anonymity property in this case may not hold.

Privacy-preserving image sharing methods. Privacy-preserving image sharing methods are designed to encrypt the content of the original image when publishing to social media. To recover the original images, the encrypted images need a key to decrypt the content. We evaluate two methods: P3 [22] and scrambling [35]. Both of them are based on the manipulation of DCT coefficients in the JPEG framework. After obtaining the DCT coefficients from 8×8 image patches, P3 separates the AC coefficients given a predefined threshold value. It then stores the coefficients that are smaller than the threshold value as the public image. The secret image contains the DC coefficients and the AC coefficients that are higher than the threshold value. In this paper, we choose the threshold value as 10. For the scrambling method, it first evenly and randomly flips the DCT coefficients and stores the result as the public image. For the secret part, it only stores the random seed. Therefore, it can restore the image by undoing the flipping process based on the random seed. In this paper, we scramble both DC and AC DCT coefficients for all YUV components, which is the high-level scrambling as proposed by [35].

B. Datasets

We use the FaceScrub dataset [18] which contains 106,863 face images from 530 identities. Therefore, the classification accuracy of randomly guessing is about 0.002. For the identification and verification attacks, we split the images from each identity into training, validation, and testing sets with the ratio of $6 : 2 : 2$. For the reconstruction attack, we split the identities into three groups for the purpose of training, validation, and testing with the same ratio. We do

---

[1] Since we fix the utility values, in this case, $x_{1,...,k}$ are the facial landmark vectors.

so to verify if the reconstruction model is able to recover unknown identity instead of just memorizing faces.

C. Obscured Face Identification Attack

Experimental Design. This attack is designed to quantify the obscuration performance in the face identification scenario. To have a more generalizable conclusion, we run the experiments based on two widely used backbone models, VGG19 and ResNet50. The input images are resized to 128×128 and the output is the softmax score for classification.

Based on the three threat models, we design the experiments as follows. In the first experiment for T_1, the identifier is trained with the set of clear images and tested with obscured images. In the second experiment for T_2, the identifier is trained on both clear and obscured images and tested with the obscured images of the obscuration method not used in the training set. The intuition of threat model T_2 is to verify if we can enforce the attacker to learn more robust features from this complex dataset. This can be seen as data augmentation. Specifically for the three traditional methods, we use the obscured images from two methods during training and use the other one for testing. For the k-same based methods and privacy-preserving image sharing methods, we train on all three traditional methods. Jointly training on clear and obscured images provides a better accuracy compared to learning from the obscured images themselves. In the third experiment for T_3, each identifier is trained on both clear and obscured images and tested with the obscured images using the same obscuration method.

Result. Table I shows the identification accuracy from different obscuration methods and threat models. The lower the identification accuracy, the better the performance of the obscuration method. The results of the clear images under T_2 and T_3 are obtained by training on all three traditional methods and testing on the clear images.

We first compare the same method and same backbone model with different threat models. As the attackers get more information (*i.e.* from T_1 to T_3), the identification accuracy increases. This means that the identifiable information left in the obscured images can still be learned by the attackers given proper training data. For example, the accuracy of Gaussian-35 with VGG19 increases from 0.007 to 0.811 for T_1 and T_3, respectively. Therefore, Gaussian blurring completely fails to provide privacy for T_3, although visually speaking a human is not able to identify someone from the obscured images. A similar conclusion can be drawn for median blurring. Although pixelation with a large pixel size can achieve a relatively good performance, comparing the results from T_1 to T_3, the attacking accuracy still improves a lot. *e.g.* for pixelation-35 with VGG19, the accuracy increases from 0.004 to 0.373, for T_1 and T_3, respectively. The three k-same based methods achieve a good obscuration performance even for T_3. For the privacy-preserving image sharing methods, although they achieve the best performance under T_1 and T_2, they still fail to provide a good obscuration under T_3. Surprisingly, even for the scrambling method which involves a random flipping process, the attackers can

still extract useful features for accurate identification. Note that these conclusions do not change for different backbone models.

Considering T_1 itself, besides Gaussian-5 and median-5, all methods achieve an effective obscuration on both VGG19 and ResNet50 models. This means that the attackers fail to extract identifiable information from the obscured images if they solely learn from the clear image. For the three traditional methods, the obscuration performance gets better (*i.e.* identification accuracy gets lower) as the kernel size increases. The original k-same method achieves the best obscuration performance among the three k-same based methods. For k-same-net and UP-GAN, since they allow the input of utility information to generate obscured faces, their obscuration performance is a little bit worse than the original k-same method. Both of the privacy-preserving image sharing methods achieve the performance of randomly guessing, which means the attackers cannot extract any identifiable information from the obscured images.

For T_2, by introducing more informative training set, all traditional methods have worse performance, besides pixelation-25 and pixelation-35, which are relatively close to the results obtained from T_1. The obscuration performance of Gaussian and median blurring drops significantly (*i.e.* the identification accuracy greatly increases). Because the two methods share similar blurring effects, the attackers can learn more robust features from the augmented training set. For the k-same based methods and privacy-preserving image sharing methods, compared to T_1, the augmented training set still does not provide useful knowledge for the attackers.

For T_3, both attackers achieve the strongest attack for all cases. Even for pixelation-35, which only contains 9 distinct pixel values, both attackers can still achieve a identification accuracy over 0.5, which is much bigger than the accuracy of randomly guessing (0.002). The three k-same based methods achieve the best obscuration performance by a great margin when compared to other methods. Surprisingly, the two privacy-preserving image sharing methods have a much worse performance compared to their performance in T_1 and T_2. Even successfully concealing the identifiable information in terms of human perception, both methods fail to provide effective obscuration.

Therefore, based on the results from the identification attack, the k-same based methods achieve the best obscuration performance.

D. Obscured Face Verification Attack

Experimental Design. Similarly to the experiment setting in the identification task, we resize the input image to 128×128. According to [3], we choose the dimension of the embedding vector as 512 and margin m as 0.5. However, if we use the re-scale factor $s = 64$ as suggested by the original paper, we are not able to obtain a stable result. Therefore, after several experiments, we empirically choose the re-scale factor as $s = 11$ for VGG19 and $s = 8$ for ResNet50, which provides the best performance according to the validation set. The batch size is chosen as 128. We

Method	Setting	Threat Model T_1		Threat Model T_2		Threat Model T_3	
		VGG19	ResNet50	VGG19	ResNet50	VGG19	ResNet50
Clear	-	0.838	0.890	0.886	0.884	0.886	0.884
Gaussian	5	0.787	0.853	0.829	0.909	0.891	0.867
	15	0.106	0.219	0.548	0.773	0.863	0.847
	25	0.010	0.030	0.236	0.573	0.830	0.819
	35	0.007	0.009	0.152	0.430	0.811	0.798
Median	5	0.786	0.855	0.883	0.907	0.913	0.907
	15	0.185	0.229	0.735	0.823	0.889	0.885
	25	0.025	0.035	0.357	0.489	0.856	0.842
	35	0.011	0.014	0.213	0.270	0.805	0.798
Pixelation	5	0.055	0.208	0.408	0.606	0.877	0.884
	15	0.004	0.003	0.008	0.008	0.651	0.643
	25	0.003	0.002	0.005	0.004	0.461	0.408
	35	0.004	0.002	0.004	0.005	0.373	0.323
k-same [7]	10	0.012	0.012	0.013	0.012	0.050	0.063
k-same-net [15]	-	0.091	0.081	0.091	0.088	0.095	0.092
UP-GAN [8]	-	0.091	0.082	0.090	0.088	0.093	0.088
P3 [22]	10	0.001	0.002	0.002	0.002	0.678	0.579
Scrambling [35]	-	0.002	0.002	0.004	0.003	0.784	0.750

TABLE I: Top-1 accuracy of the identification attack. The method *Clear* means the identification of the clear image. The lower the accuracy, the better the obscuration method.

Method	Setting	Threat Model T_1		Threat Model T_2		Threat Model T_3	
		VGG19	ResNet50	VGG19	ResNet50	VGG19	ResNet50
Clear	-	0.984	0.979	0.984	0.978	0.984	0.978
Gaussian	5	0.984	0.978	0.981	0.979	0.982	0.977
	15	0.927	0.917	0.970	0.961	0.960	0.972
	25	0.674	0.735	0.880	0.910	0.968	0.968
	35	0.561	0.623	0.799	0.860	0.963	0.963
Median	5	0.981	0.975	0.982	0.978	0.982	0.979
	15	0.749	0.753	0.933	0.944	0.933	0.970
	25	0.618	0.627	0.830	0.891	0.876	0.962
	35	0.535	0.573	0.557	0.770	0.804	0.954
Pixelation	5	0.795	0.833	0.906	0.899	0.979	0.973
	15	0.504	0.518	0.755	0.659	0.889	0.917
	25	0.504	0.511	0.521	0.537	0.817	0.862
	35	0.503	0.505	0.507	0.517	0.591	0.780
k-same [7]	10	0.528	0.519	0.528	0.524	0.648	0.662
k-same-net [15]	-	0.553	0.554	0.550	0.552	0.511	0.550
UP-GAN [8]	-	0.554	0.554	0.549	0.549	0.511	0.520
P3 [22]	10	0.501	0.501	0.501	0.500	0.878	0.947
Scrambling [35]	-	0.503	0.515	0.505	0.515	0.954	0.966

TABLE II: AUC ROC for the verification attack. The lower the AUC, the better the obscuration method.

choose the stochastic gradient descent (SGD) as optimizer with a weight decay of $5e^{-4}$. The learning rate starts at 0.1 and is divided by 10 at the epochs of 6, 11, and 16. For the training of P3 and scrambling, we reduce the starting learning rate to 0.05 due to convergence issues. Assuming the identification task, we implement the experiments based on the three threat models. For the performance metric, since the face verification problem is just a binary classification problem, we choose the area under the curve (AUC) of the receiver operating characteristic (ROC) curve to examine the performance.

During testing we need to obtain pairs of faces with the same identity and pairs of faces with different identities. Due to the large number of combinations of valid pairs from the testing set, in our implementation, we only compute all valid pairs within each mini-batch (128 images which are coming from 64 identities). Furthermore, we run testing 10 times with different combinations of image pairs. The average AUC is been reported in Table II. The standard deviation for the tests ranges from $[0.003, 0.037]$. Therefore, we can directly use the average AUC to compare different experiments because of the small variation.

Result. Table II shows the verification AUC from different obscuration methods, threat models and backbone models. The lower the AUC, the better the performance of the obscuration method. We first compare the same method and same backbone model to different threat models. As the attackers get more information (from T_1 to T_3), the verification AUC increases. Take Gaussian-35 with VGG19 as an instance again. The AUC increases from 0.561 to 0.963 for T_1 and T_3, respectively. Note that the AUC for randomly guessing is 0.5. This means that although Gaussian-35 can successfully defend from the attack under T_1, after introducing the obscured data in the training set, the

attackers can still extract enough identifiable information to achieve a high accuracy verification. For the k-same based methods, similar to the identification attack, they achieve a robust obscuration performance even for T_3. For the privacy-preserving image sharing methods, both of them succeed in T_1 and T_2, but fail to obscure the identities under T_3. Note that for different backbone models, although there is a small performance difference, choosing different models does not affect the conclusions reached above.

Consider different methods with the same threat model and backbone model. For the traditional methods, a similar conclusion to the identification attack can be drawn. As the kernel (pixel) size increases, the AUC decreases for all cases, especially for pixelation-35 with VGG19 which achieves the best performance among the traditional methods. The k-same based methods achieve good results for all threat models and both attackers, which agrees with the conclusion from the identification attack. Although the privacy-preserving image sharing methods can conceal identities well under T_1 and T_2, for the stronger T_3, both of them fail to provide effective obscuration.

Therefore, based on the results from the verification attack, the k-same based methods achieve the best obscuration performance.

E. Obscured Face Reconstruction Attack

Method	Setting	MSE↑	Accuracy↓
Clear	-	0.000	0.849
Gaussian	5	0.000	0.824
	15	0.001	0.707
	25	0.002	0.519
	35	0.002	0.367
Median	5	0.001	0.774
	15	0.003	0.356
	25	0.004	0.152
	35	0.007	0.102
Pixelation	5	0.004	0.439
	15	0.014	0.043
	25	0.022	0.013
	35	0.031	0.006
k-same [7]	10	0.029	0.005
k-same-net [15]	-	0.064	0.018
UP-GAN [8]	-	0.059	0.003
P3 [22]	10	0.013	0.339
Scrambling [35]	-	0.018	0.042

TABLE III: MSE and identification accuracy of the reconstruction attack. The arrows next to *MSE* and *Accuracy* indicate that the higher the MSE and the lower the identification accuracy are, the better the obscuration method is.

Experimental Design. In the previous sections we show that most of the obscuration methods fail to remove all identifiable information. In this reconstruction attack, we try to use the remaining information from these obscured images to recover the clear image. If the remaining information has a strong correlation with the information from the clear image, we should be able to reconstruct the original face with a high accuracy. In this implementation, we choose Pix2Pix

[10] which is a GAN model designed for image-to-image translation as our reconstruction model.

Assume that the obscured images and clear images come from two distinct distributions. The reconstruction model aims to find a mapping function from the obscured image distribution to the clear image distribution. To quantify the reconstruction performance, we choose mean square error (MSE) as the metric to calculate pixel-wise distance between the clear image and the reconstructed image. The value range of the clear image and reconstructed image is $[0, 1]$. To evaluate similarity of the identifiable information from the reconstructed image and the clear image, we use the identification accuracy obtained from the ResNet50 model which is pretrained on the clear images. This is the same setting as T_1, since the attacker is trained with clear images and tested with obscured images.

Result. Figure 1 shows the reconstruction results from Gaussian-25, median-25, pixelation-25, P3, scrambling, k-same, k-same-net, and UP-GAN. Visually, the three k-same based methods can successfully prevent reconstruction compared with other methods. Although the privacy-preserving image sharing methods can prevent identification in terms of human perception, the reconstruction model can still recover the images fairly accurately, especially for P3. For the three traditional methods, pixelation-25 achieves a better obscuration performance compared to Gaussian-25 and median-25.

Table III shows the results of the face reconstruction attack. Note that setting *Clear* means we input clear images to Pix2Pix model to achieve an identity mapping. The exact MSE for the clear image is 0.000144 and the exact MSE for Gaussian-5 is 0.000289. For the three traditional methods, with the kernel (pixel) size increases, the reconstruction MSE increases and the identification accuracy decreases. Compared to the identification attack of T_1, this reconstruction process can help the attackers achieve a stronger attack, since the accuracy from the reconstructed images is higher than the obscured images for most cases. The k-same based methods achieve both high MSE and low identification accuracy. Compared to the three k-same methods, the two privacy-preserving image sharing methods are vulnerable to the reconstruction attack, because of their low MSE. Therefore, as with the conclusion in the identification and verification attack, these two methods also fail to conceal identity on this reconstruction attack.

V. CONCLUSION

In this paper, we propose a set of experiments to analyze the robustness of face obscuration methods. We provide a comprehensive analysis of eight obscuration methods: Gaussian blurring, median blurring, pixelation, k-same, k-same-net, UP-GAN, P3, and scrambling. We examine the robustness of these methods under different attacking scenarios including identification, verification, and reconstruction with two widely used deep learning models, VGG19 and ResNet50. Threat modeling is also considered to evaluate the obscuration methods under different strength of attacks.

Methods such as Gaussian blurring, median blurring, P3, and scrambling fail to provide an effective obscuration under the designed attackers, although they successfully defeat human perception. We also show that the k-same based methods can provide a secured privacy protection. Hence, since relying on human perception is no longer an option to guarantee privacy, the proposed set of experiments should be used to quantify and benchmark the effectiveness of any future face obscuration method.

References

[1] Q. Cao, L. Shen, W. Xie, O. M. Parkhi, and A. Zisserman. VggFace2: A dataset for recognising faces across pose and age. *Proceedings of the International Conference on Automatic Face and Gesture Recognition*, May 2018. Xi'an, China.

[2] T. F. Cootes, G. J. Edwards, and C. J. Taylor. Active appearance models. *IEEE Transactions on Pattern Analysis and Machine Intelligence*, 23(6):484–498, June 2001.

[3] J. Deng, J. Guo, N. Xue, and S. Zafeiriou. ArcFace: Additive angular margin loss for deep face recognition. *Proceedings of the IEEE International Conference on Biometrics Theory, Applications and Systems*, June 2019. Long Beach, CA.

[4] L. Du, M. Yi, E. Blasch, and H. Ling. Garp-Face: Balancing privacy protection and utility preservation in face de-identification. *Proceedings of the IEEE International Joint Conference on Biometrics*, pages 1–8, September 2014. Clearwater, FL.

[5] F. Dufaux and T. Ebrahimi. A framework for the validation of privacy protection solutions in video surveillance. *Proceedings of the IEEE International Conference on Multimedia and Expo*, pages 66–71, July 2010. Singapore, Singapore.

[6] I. Goodfellow, J. Pouget-Abadie, M. Mirza, B. Xu, D. Warde-Farley, S. Ozair, A. Courville, and Y. Bengio. Generative adversarial nets. *Proceedings of Advances in Neural Information Processing Systems*, pages 2672–2680, December 2014. Montréal, Canada.

[7] R. Gross, E. Airoldo, B. Malin, and L. Sweeney. Integrating utility into face de-identification. *Proceedings of the International Workshop on Privacy Enhancing Technologies*, pages 227–242, May 2005. Cavtat, Croatia.

[8] H. Hao, D. Güera, A. R. Reibman, and E. J. Delp. A utility-preserving gan for face obscuration. *Proceedings of the International Conference on Machine Learning, Synthetic Realities: Deep Learning for Detecting AudioVisual Fakes Workshop*, June 2019. Long Beach, CA.

[9] K. He, X. Zhang, S. Ren, and J. Sun. Deep residual learning for image recognition. *Proceedings of the IEEE Conference on Computer Vision and Pattern Recognition*, pages 770–778, June 2016. Las Vegas, NV.

[10] P. Isola, J.-Y. Zhu, T. Zhou, and A. A. Efros. Image-to-image translation with conditional adversarial networks. *Proceedings of the IEEE Conference on Computer Vision and Pattern Recognition*, pages 5967–5976, June 2016. Las Vegas, NV.

[11] D. E. King. Dlib-ml: A machine learning toolkit. *Journal of Machine Learning Research*, 10:1755–1758, December 2009.

[12] W. Liu, Y. Wen, Z. Yu, M. Li, B. Raj, and L. Song. SphereFace: Deep hypersphere embedding for face recognition. *Proceedings of the IEEE Conference on Computer Vision and Pattern Recognition*, pages 6738–6746, July 2017. Hawaii, HI.

[13] W. Liu, Y. Wen, Z. Yu, and M. Yang. Large-margin softmax loss for convolutional neural networks. *Proceedings of the International Conference on Machine Learning*, pages 507–516, June 2016. New York, NY.

[14] R. McPherson, R. Shokri, and V. Shmatikov. Defeating image obfuscation with deep learning. *arXiv:1609.00408v2*, September 2016.

[15] B. Meden, Ž. Emeršič, V. Štruc, and P. Peer. k-same-net: k-anonymity with generative deep neural networks for face deidentification. *Entropy*, 20(1), January 2018.

[16] M. Mirza and S. Osindero. Conditional generative adversarial nets. *arXiv:1411.1784v1*, November 2014.

[17] E. M. Newton, L. Sweeney, and B. Malin. Preserving privacy by de-identifying face images. *IEEE Transactions on Knowledge and Data Engineering*, pages 232–243, Feburary 2005.

[18] H. Ng and S. Winkler. A data-driven approach to cleaning large face datasets. *Proceedings of the IEEE International Conference on Image Processing*, pages 343–347, October 2014. Paris, France.

[19] S. J. Oh, R. Benenson, M. Fritz, and B. Schiele. Faceless person recognition: Privacy implications in social media. *Proceedings of European Conference on Computer Vision*, pages 19–35, January 2016. Amsterdam, The Netherlands.

[20] C. Pares-Pulido and I. Agudo. Lockpic: Privacy preserving photo sharing in social networks. *Proceedings of the International Workshop on Data Privacy Management, and Security Assurance*, pages 281–290, September 2016. Heraklion, Crete.

[21] O. M. Parkhi, A. Vedaldi, and A. Zisserman. Deep face recognition. *Proceedings of British Machine Vision Conference*, pages 41.1–41.12, September 2015. Swansea, UK.

[22] M.-R. Ra, R. Govindan, and A. Ortega. P3: Toward privacy-preserving photo sharing. *Proceedings of the USENIX Symposium on Networked Systems Design and Implementation*, pages 515–528, April 2013. Lombard, IL.

[23] S. Sah, A. Shringi, R. Ptucha, A. M. Burry, and R. P. Loce. Video redaction: a survey and comparison of enabling technologies. *Journal of Electronic Imaging*, 26(5):1 – 14 – 14, July 2017.

[24] P. Samarati and L. Sweeney. k-anonymity: a model for protecting privacy. *International Journal of Uncertainty, Fuzziness and Knowledge-Based Systems*, 10(5):557–570, October 2002.

[25] S. Sankaranarayanan, A. Alavi, C. D. Castillo, and R. Chellappa. Triplet probabilistic embedding for face verification and clustering. *Proceedings of the IEEE International Conference on Biometrics Theory, Applications and Systems*, pages 1–8, September 2016. Buffalo, New York.

[26] F. Schroff, D. Kalenichenko, and J. Philbin. FaceNet: A unified embedding for face recognition and clustering. *Proceedings of the IEEE Computer Vision and Pattern Recognition*, pages 815–823, June 2015. Boston, USA.

[27] K. Simonyan and A. Zisserman. Very deep convolutional networks for large-scale image recognition. *Proceedings of the International Conference on Learning Representations*, May 2015. San Diego, CA.

[28] Y. Sun, Y. Chen, X. Wang, and X. Tang. Deep learning face representation by joint identification-verification. *Proceedings of Advances in Neural Information Processing Systems*, pages 1988–1996, December 2014. Montréal, Canada.

[29] Y. Sun, X. Wang, and X. Tang. Deep learning face representation from predicting 10,000 classes. *Proceedings of the IEEE Conference on Computer Vision and Pattern Recognition*, pages 1891–1898, June 2014. Washington, DC.

[30] Y. Sun, X. Wang, and X. Tang. DeepID3: Face recognition with very deep neural networks. *arXiv:1502.00873*, Feburary 2015.

[31] Y. Sun, X. Wang, and X. Tang. Deeply learned face representations are sparse, selective, and robust. *Proceedings of the IEEE Conference on Computer Vision and Pattern Recognition*, pages 2892–2900, June 2015. Boston, MA.

[32] Y. Taigman, M. Yang, and L. Wolf. Deepface: Closing the gap to human-level performance in face verification. *Proceedings of the IEEE International Conference on Biometrics Theory, Applications and Systems*, pages 1701–1708, June 2014.

[33] F. Wang, J. Cheng, W. Liu, and H. Liu. Additive margin softmax for face verification. *IEEE Signal Processing Letters*, 25(7):926–930, July 2018.

[34] H. J. Wang, Y. Wang, Z. Zhou, X. Ji, D. Gong, J. Zhou, Z. Li, and W. Liu. Cosface: Large margin cosine loss for deep face recognition. *Proceedings of the IEEE Conference on Computer Vision and Pattern Recognition*, pages 5265–5274, June 2018. Salt Lake City, UT.

[35] L. Yuan, P. Korshunov, and T. Ebrahimi. Privacy-preserving photo sharing based on a secure jpeg. *Proceedings of the IEEE Conference on Computer Communications Workshops*, pages 185–190, April 2015. Hong Kong, China.

[36] Z. Zhang, Y. Song, and H. Qi. Age progression/regression by conditional adversarial autoencoder. *Proceedings of the IEEE Conference on Computer Vision and Pattern Recognition*, pages 4352–4360, July 2017. Hawaii, HI.